Available online at www.sciencedirect.com

ScienceDirect

Journal of Taibah University for Science 10 (2016) 430–436

Journal of Taibah University for Science

www.elsevier.com/locate/jtusci

Global minima of iron clusters described by Gupta potential

S. Nouemo *, F. Tchoffo, J.M.B. Ndjaka, S. Domngang

Department of Physics, Faculty of Sciences, University of Yaounde I, P.O. Box 812, Yaounde, Cameroon

Received 30 May 2014; received in revised form 19 May 2015; accepted 29 June 2015
Available online 2 December 2015

Abstract

In this paper, we present global minimum energy for iron clusters, ranging from sizes $N=2$ to 100 atoms, described by the phenomenological Gupta potential. Our optimized structures and symmetry groups are in agreement with previous ones obtained using Finnis–Sinclair potential; but our energy levels and nearest neighbor distances differ slightly. The origins of the differences are related back to the differences in the potentials.

Keywords: Iron clusters; Gupta potential; Global optimization

1. Introduction

The behavior and characteristics of condensed matter systems are controlled by their structure, since mechanical, transport, optical, chemical land magnetic properties are determined by them. Thus, establishing the way, the constituent atoms arrange spatially to form molecules, nanoclusters and crystals, is the fundamental problem of solid state physics [1]. Nanoclusters are aggregates that contain up to million atoms and constitute the building blocks of nanoscience; the structure of transition metal nanoclusters (with diameters between 1 and 10 nm) is of significant theoretical and practical interest due to their potential use in ultrahigh density magnetic recording materials [2], catalytic particles in the synthesis of carbon nanotubes [3,4] and other applications in electronics and optics. Due to their small size, nanoclusters can remain in a "liquid-like" state at temperatures well below the bulk melting point [5,6], and their magnetic moments can exceed bulk value up to cluster sizes of several hundred atoms [7]. In general, the geometric structures of the clusters do not resemble those of the bulk metals since there are no constraints on rotational symmetry from the crystallographic restriction theorem. The structure of an iron cluster is one of its most important properties, yet it is a property that can be hard to access for clusters.

Computer simulations are carried out in the hope of understanding the properties of assemblies of molecules in terms of their structure and the microscopic interactions between them.

This serves as a complement to conventional experiments, usually leading only to an indirect measurement of the structure; consequently, experimental results need to be compared to what would be expected for candidate structures. The experimental procedures have been successful isolating the larger species of fullerenes and

* Corresponding author. Tel.: +237 677164979.
E-mail address: nouem_s@yahoo.com (S. Nouemo).
Peer review under responsibility of Taibah University.

Production and hosting by Elsevier

http://dx.doi.org/10.1016/j.jtusci.2015.06.014

determining their geometries. However, sophisticated global minimization techniques have been developed and implemented in order to find the lowest energy configuration among a huge number of local minima [1,8–10]. Given the complexity of the problem (for example, the potential energy surface of 13 atom Lennard–Jones cluster has about a thousand of minima [10]), it is not surprising that some degree of controversy and uncertainty are always present. The ground state structure of small clusters is still not known with certainty and many isomers structure have been proposed.

The lowest energy structure of cluster can be determined using ab-initio electronic structure methods. But when the number of atoms constituent the cluster becomes high, ab-initio calculations which are very time consuming. Therefore, several semi-empirical potentials [11–13] which describe correctly the interactions amongst cluster atoms, have been developed. For accurate determination of energy, the potential must incorporate: well modeled different external surfaces, twin planes, different crystal structures, and the response to strain. To model the potential temperature dependence of the structure, vibrational properties need also to be well described [14]. Therefore, prediction of the correct structure of a cluster represents a tough challenge for a potential in use. Furthermore, it is often not clear which of the available potentials will work better for a considered system. Even using some semi-empirical potentials to determine the minimal configurations of structures, the convergence is not always guaranteed particularly when the number of atoms constituent the structure becomes high.

The objectives of this study are to use the phenomenological many-body Gupta potential to determine the lowest energy structure of all Fe_N clusters in the range $2 \leq N \leq 100$. Thereafter we compare our results with those obtained using Finnis–Sinclair (SE-MO and Lennard–Jones) [15] potentials. The most important fact in the Gupta potential is that for a sufficiently long time, it converges directly toward the optimized structure and this occurs whatever be the initial configuration. Consequently, this method can allow one to simulate systems much larger than previously accessible, widening the range of materials science issues that can be addressed. Gupta potential allows one to perform simulations involving up to three hundred of atoms on small work stations. This type of potential has been extensively used in metallic cluster simulations [16,17], and it leads to results that are in good agreement with those generated from first-principles methods [18]. We work in a similar spirit as Refs. [12,14,19], where possible structural patterns for sodium, aluminum, zinc and cadmium clusters modeled by the Gupta potential have been suggested.

The paper is organized as follows: In Section 2, we describe the model potential and provide details on the simulation method. In Section 3, total energy behavior and some of the global minimum cluster structures obtained from our calculations are presented and compared with those obtained using FS potentials and SE-MO theory. A summary of this work is presented in Section 4.

2. Potential and methodology

2.1. Potential description

The many-body model potential used in this work is the semi-empirical Gupta potential [20–22] which was derived from Gupta's expression for cohesive energy of bulk material [21] and is based on the second moment approximation of a tight-binding Hamiltonian [21]. The interaction between the iron atoms in the long distance was disregarded. The cohesive energy of the system depends on five parameters, and is written in terms of repulsive pair and attractive many body terms which are obtained by summation over all atoms and it is expressed by the summation of the total bonding energy between two atoms as follows:

$$E = A\sum_{i=1}^{N}\sum_{j>i}^{N} e^{p\left(1-\frac{r_{ij}}{r_0}\right)} - \xi\sum_{i=1}^{N}\sqrt{\sum_{i=1}^{N} e^{2q\left(1-\frac{r_{ij}}{r_0}\right)}} \qquad (1)$$

where r_{ij} is the interatomic distance between atoms i and j; r_0, A, ξ, p and q are adjustable parameters that represent, respectively, the equilibrium Fe–Fe bond, the repulsive coefficient, the attractive coefficient, and the last two denote the range of the interaction [21]. The parameters of the Gupta potential that we used are shown in Table 1.

2.2. Methodology

All the global optimization calculations in the work were performed using a numerical code based on the constant-energy molecular dynamics method. We have calculated the structural changes as a function of the cluster energy. Within this method, Newton's equations of motion are solved for each atom within the cluster using

Table 1
Gupta parameters for iron cluster.

$A = 9.6000$ eV	$p = 4.5000$	$\xi = 1.8000$ eV	$q = 0.4000$

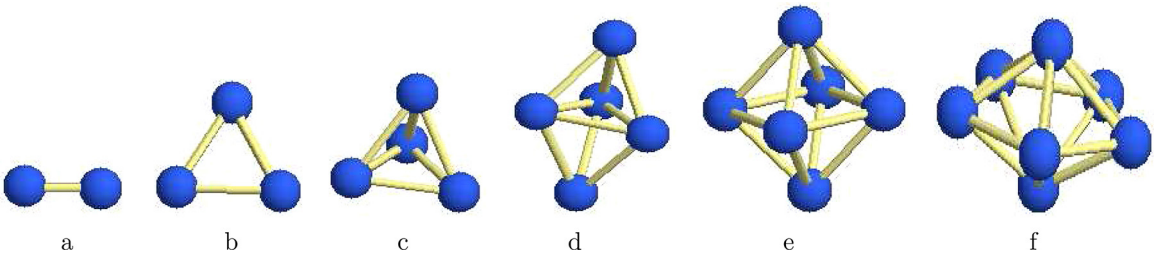

Fig. 1. Different Gupta optimized configurations of Fe: (a) Fe_2, (b) Fe_3, (c) Fe_4, (d) Fe_5, (e) Fe_6 and (f) Fe_7.

the Verlet algorithm [23]. r_0 is used as the bond unit and a time step is set of 0.05 fs. Through this procedure, we obtained the atomic positions and momenta as a function of time that are used to calculate time-averages of physical quantities characterizing the cluster structure and dynamics. To simulate this procedure, the cluster total energy is increased in a step-like manner by scaling up the atomic velocities and therefore increasing the kinetic energy of the cluster. The initial configurations used to start our calculations were: line, cage, circle, cylinder, bowl and butterfly and the initial velocities of each atom were chosen randomly.

3. Results and discussion

To set Gupta potential parameters listed in Table 1, we have determined the optimal configurations of Fe_2, Fe_3, Fe_4, Fe_5, Fe_6 and Fe_7 which are mostly discussed in literature. The optimized configurations are shown in Fig. 1a, b, c, d, e and f, respectively.

We started our verifications with Fe_2 cluster, the bond length in iron dimer Fe_2 is $2.1105r_0$.

The total energy is -2.4368 eV. The results are in good agreement with many other results such as those obtained by Chen et al. [24] using LSDA method and Calaminici [25] based on a DFT calculation.

There are controversies about the assignment of the ground-state structure for Fe_3 cluster.

Most previous DFT calculations on Fe_3 [24,26–29] proposed an equilateral triangle. Gutsev and Bauschlicher [30] have predicted an isosceles triangle as ground state. In our computational study, we have tested all possible geometric initial configurations for Fe_3 cluster and we found that the lowest-energy structure is the D_{3h} structure with a total energy equal to -4.9741 eV. The value of bond length is $2.1749r_0$. These results agree well with those obtained by Ma et al. [31].

Most theoretical calculations for Fe_4 have predicted that the most stable isomer is a regular [24,25] or distorted [26,27] tetrahedron. In the present work, we found that the T_d structure is the most stable one. Ballone and Jones [27] found the same results by molecular dynamics simulations. Elsewhere, Yuan et al. [32], starting from a free regular tetrahedral structure, have obtained the distorted tetrahedral structure (D_{2d} symmetry) as the ground state.

For Fe_5, four configurations are found and tested such as ring, pyramid, bitetrahedron and line. The most stable of them is bitetrahedron structure (D_{3h}). Here, we found excellent agreement with several studies [33]. But the authors of reference [24] show that C_{2v} is the most stable structure for Fe_5.

In the case of Fe_6 cluster, two geometries seem to be as the most stable possible configurations. From our simulations, we found that the regular octahedron is the most stable structure. The obtained results contradict the results of Ballon et al. [27] who found that capped trigonal bipyramid is the minimum energy structure, but agrees with that of Gutsev and Bauschlicher [30] and Dieguez et al. [28].

In the literature, three stable structures are obtained for Fe_7 cluster: D_{2h}, C_{3v} and the C_s geometries. Our results for Fe_7 can be compared with those obtained by Dieguez et al. [28] and Kohler et al. [29]. Similar results are obtained elsewhere [27,33].

We have found that, in this way, practically all global energy minimum structures of the Gupta clusters can be determined. Table 2 depicts the potential energy, Group Point and Fe–Fe bond of all the clusters.

In this table, structural assignment has been made, where *C* stands for cyclic, *D* for decahedral, *I* for icosahedral, *T* for tetrahedron and *O* for octahedron. For the Lennard–Jones potential, major part of the structures is based upon the icosahedron [15]. Whereas for the Gupta and Finnis–Sinclair potentials, major part of the structures is cyclic [15].

We have obtained from our simulations, 14 symmetry groups: D_{3h}, T_d, O_h, D_{5h}, C_1, C_s, C_{2v}, C_2, C_{3v}, C_{5v}, C_{6v}, D_{3d}, D_{6h} and I_h. In any symmetry group, we have chosen one molecule and their structures of the global minima are depicted in Fig. 2. In order with symmetry groups given above, structures of Fe_8, Fe_9, Fe_{10}, Fe_{12}, Fe_{13},

Table 2
Potential and bonds of the lowest energy configurations.

N	Energy (eV)	Bond	PG	N	Energy (eV)	Bond	PG	N	Energy (eV)	Bond	PG
2	−2.4368	2.1105	D_{1h}	3	−4.9741	2.1749	D_{3h}	4	−7.9418	2.2126	T_d
5	−10.8737	2.2037	D_{3h}	6	−14.1493	2.2264	O_h	7	−17.2500	2.2014	D_{5h}
8	−20.2295	2.1669	C_s	9	−23.6530	2.1992	C_{2v}	10	−27.0829	2.1726	C_{3v}
11	−30.5402	2.1495	C_{2v}	12	−34.3799	2.1536	C_{5v}	13	−38.5805	2.1790	I_h
14	−41.6170	2.1728	C_{3v}	15	−45.0923	2.1629	C_{2v}	16	−48.5703	2.1715	C_s
17	−51.9703	2.1125	C_s	18	−55.80361	2.0507	C_s	19	−60.0260	2.0331	D_{5h}
20	−63.5430	2.0301	C_{2v}	21	−67.0127	2.0385	C_1	22	−70.7402	2.0611	C_s
23	−74.9649	2.0718	D_{3h}	24	−78.4581	2.0606	C_{2v}	25	−81.9285	2.0294	C_{2v}
26	−86.3807	2.1014	T_d	27	−89.8459	2.0657	C_{2v}	28	−93.6107	2.0699	C_s
29	−97.7272	2.0926	D_{3h}	30	−101.2374	2.0580	C_{2v}	31	−104.9838	2.0599	C_s
32	−109.0569	2.0836	C_{2v}	33	−112.5079	2.0328	C_s	34	−116.7926	2.0815	D_{5h}
35	−120.3225	2.0547	C_2	36	−123.8160	2.0304	C_s	37	−127.8610	2.0233	C_s
38	−131.5208	2.0172	D_{6h}	39	−135.9637	2.0230	C_{6v}	40	−140.2138	2.0195	D_{6h}
41	−143.8140	2.0184	C_s	42	−147.3749	2.02001	C_s	43	−150.8132	1.9985	C_s
44	−156.0294	2.0084	C_{2v}	45	−159.5931	2.0187	C_s	46	−164.0024	2.0424	C_s
47	−167.5049	1.9892	C_s	48	−172.1718	2.0434	C_{3v}	49	−186.1994	1.9062	C_s
50	−179.4050	2.0242	C_1	51	−183.7756	2.0250	C_s	52	−187.7215	2.0287	C_s
53	−191.9613	2.0248	C_s	54	−195.4263	2.0049	D_{3h}	55	−199.3533	2.0045	C_s
56	−204.1003	2.0376	C_s	57	−207.5300	2.0032	T_d	58	−212.0088	2.0065	C_{3v}
59	−216.4708	2.0106	C_{2v}	60	−220.9081	2.0151	C_{3v}	61	−225.2980	2.0184	T_d
62	−227.7495	1.9932	C_s	63	−232.1919	1.9970	C_s	64	−236.5857	1.9990	C_{3v}
65	−239.0030	1.9741	C_{2v}	66	−243.4492	1.9768	C_s	67	−247.7869	2.0080	C_1
68	−252.2265	2.0013	C_s	69	−256.1579	2.0165	C_s	70	−260.6207	2.0178	C_s
71	−263.7196	2.0050	C_s	72	−268.1983	2.0098	C_s	73	−272.4957	2.0113	C_1
74	−277.0341	2.0190	C_s	75	−279.7447	2.0031	C_s	76	−285.8283	2.0367	D_{6h}
77	−290.1599	2.0149	C_{6v}	78	−294.4091	1.9821	D_{6h}	79	−296.7802	2.0038	C_s
80	−301.2379	2.0104	C_2	81	−305.6715	2.0109	C_s	82	−310.0907	2.0172	D_{3d}
83	−314.0370	1.9925	C_{2v}	84	−317.8132	1.9841	C_2	85	−321.8199	2.0066	C_{2v}
86	−326.1248	2.0258	C_1	87	−330.4583	2.0213	C_1	88	−334.6796	1.9948	C_1
89	−338.7875	1.9879	C_s	90	−343.0390	2.0140	C_1	91	−346.7808	2.0144	C_1
92	−350.4326	2.0033	C_s	93	−356.1342	2.0247	C_{2v}	94	−359.3768	2.0137	C_s
95	−363.1956	2.0193	C_1	96	−367.3012	2.0111	C_1	97	−371.4273	2.0026	C_1
98	−375.8534	2.0197	C_1	99	−379.7859	1.99454	C_s	100	−383.8792	1.9859	C_1

Fe_{35}, Fe_{38}, Fe_{39}, Fe_{67} and Fe_{82} are plotted in Fig. 2a, b, c, d, e, f, g, h, i and j, respectively, since the following structures Fe_3, Fe_4, Fe_6 and Fe_7 have been already drawn in Fig. 1.

For Fe_{13} and Fe_{19}, Elliot et al. [15] using Finis–Sinclair potential obtained simple and double icosahedra in common with Lennard–Jones (12–6) some Sutton–Chen (12–6, 9–6) and some Gupta (Na, Co) clusters of the same size and for Gupta Fe_{13} and Fe_{19} we obtained the same result as the authors of Ref. [15]. For Fe_{23} the predicted global minimum structure by Finis–Sinclair is different from a Sutten–Chen (9,6) cluster with point group C_2.

As shown in Table 2, the ground state energy decreases with the number N of atoms. In order to go far in our analysis, we plot on Fig. 3 the ground state energy as function of N (curve with dots). This curve brings the following analysis: the shape of the curve is almost linear and then can be approximated by the following relation.

$$\text{Energy} \simeq aN + b \tag{2}$$

By using linear regression method we obtain: $a = -3.9558$ eV, $b = 15.4926$ eV. To verify our assumption, we have plotted on Fig. 3 (curve with solid line) the above relation. A good agreement is obtained here between numerical result and semi-analytical one. The result obtained in Eq. [2] is an important relation because this can help in the prediction of the shape, symmetry and properties of an unknown iron cluster and its ground state energy knowing N and without numerical simulation.

On the other hand, the distances between the nearest Fe–Fe iron atoms remain almost constant as shown in Fig. 4. We observe that in the range 2–30 atoms, clusters with 20 and 25 atoms have the smallest Fe–Fe bound,

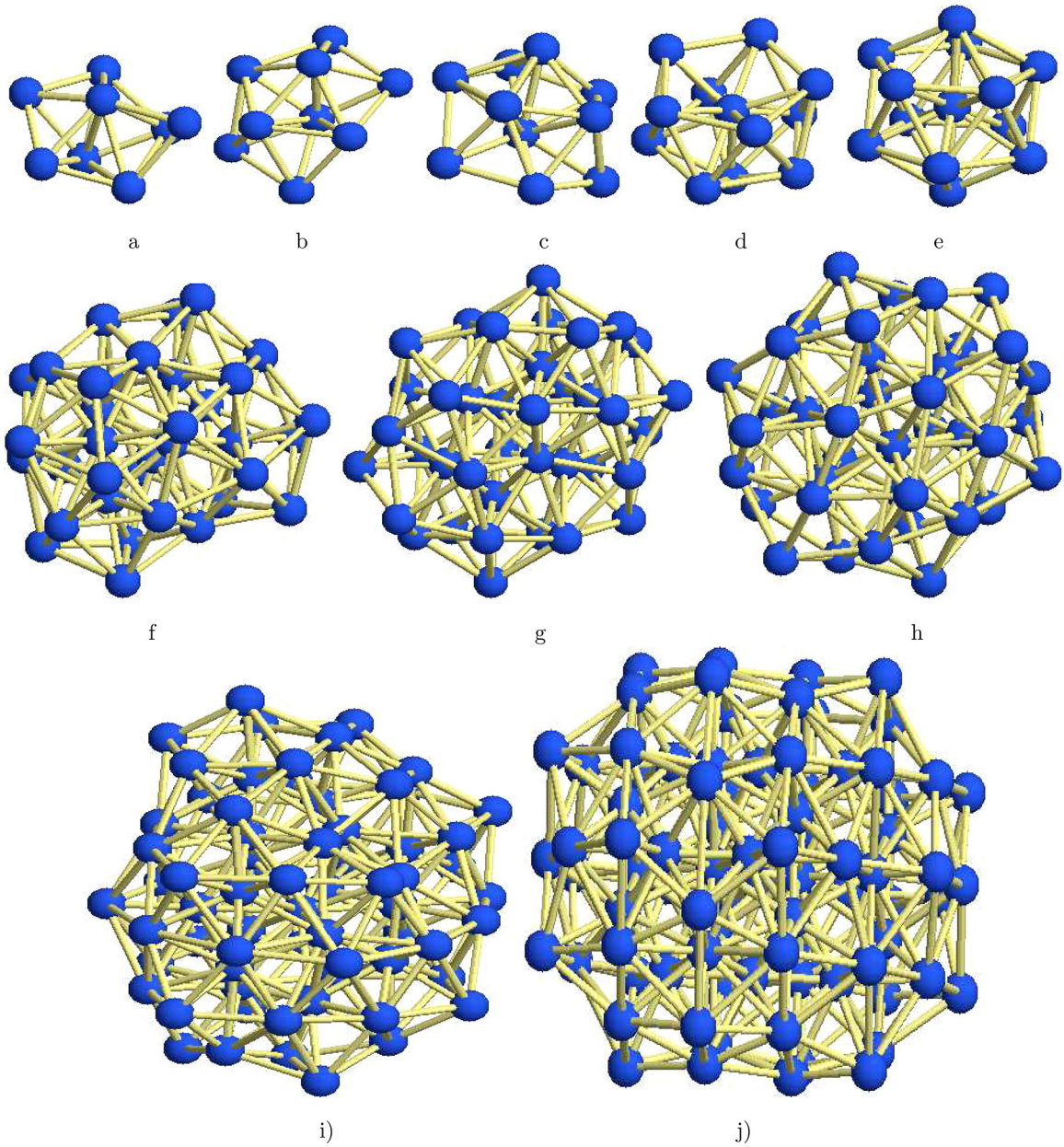

Fig. 2. Different Gupta optimized configurations of Fe: (a) Fe_8, (b) Fe_9, (c) Fe_{10}, (d) Fe_{12}, (e) Fe_{13}, (f) Fe_{35}, (g) Fe_{38}, (h) Fe_{39}, (i) Fe_{67} and (j) Fe_{82}.

from 31 to 60, clusters that have smallest Fe–Fe bound are those with 43 and 47 atoms while, from 61 to 100 atoms the lowest Fe–Fe bound is attributed to clusters of 65, 68 and 78 atoms.

Our results show that the higher Fe–Fe distance is obtained in the case of Fe_6 cluster while Fe_{65} cluster has the lower distance. The geometrical structures found in the present work agree well with other calculations, particularly, our simulations give the same optimized configurations as Ref. [15]. In comparison with C_{20}, we aim to verify whether Fe_{20} cluster has fullerene structure as another stable configuration or isomer; but it is not the case with Gupta potential; the optimized structure of Fe_{20} is not a fullerene. From different initials configurations shown in Fig. 5, we have obtained the same final optimized configuration that has energy -63.5430 eV. The minimum distance between Fe_{20} atoms is approximately constant and very close to $2.0301 r_0$.

The only difference here is the time taken by each initial configuration to reach the optimized configuration.

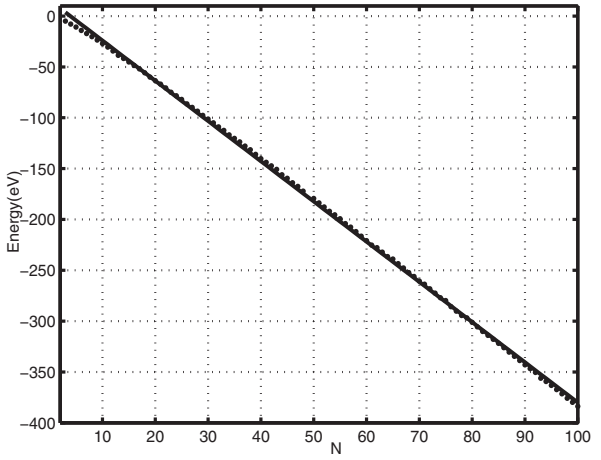

Fig. 3. Ground state energy as function of the number of atoms: curve with dots is our simulation result while solid line represents the approximated curve by relation [2].

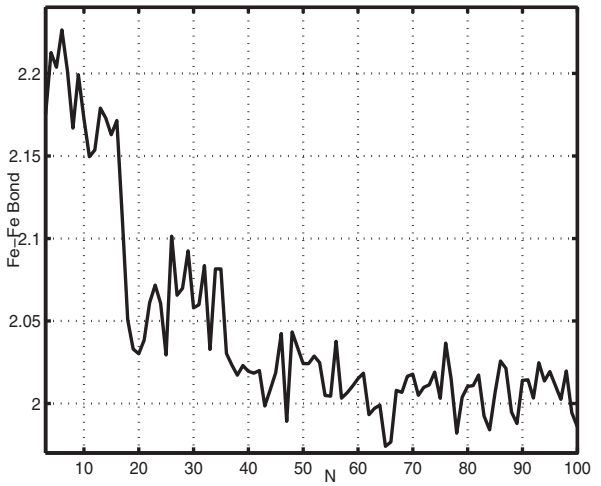

Fig. 4. Fe–Fe bond as function of the number of atoms.

Because of its symmetry, the butterfly configuration shown in Fig. 5b is the one which takes more time ($t = 47{,}089$) followed by the bowl configuration ($t = 43{,}535$). The following configurations: cage (Fig. 5a) and cylinder (Fig. 5c) stabilized respectively at $t = 38{,}295$ and $t = 32{,}105$. The optimized configuration is represented in Fig. 6.

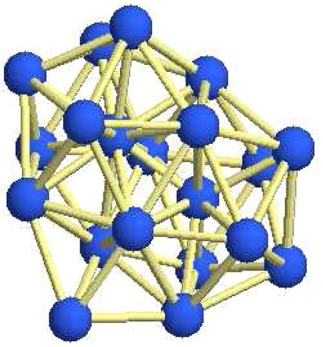

Fig. 6. Optimized configuration of Fe_{20}.

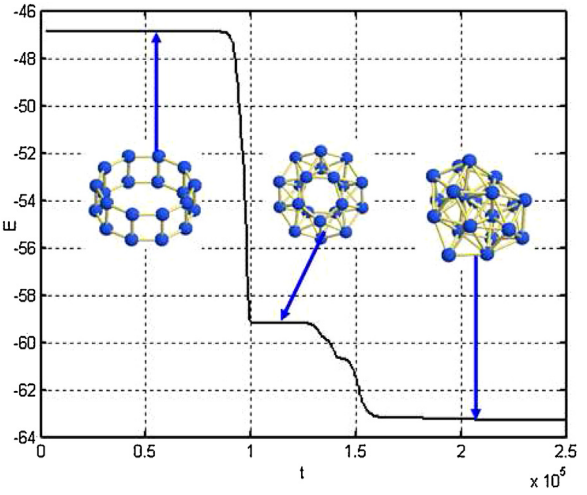

Fig. 7. An illustration of the evolution of the lowest-energy Fe_{20} molecule with the Gupta potential starting from a cylinder configuration.

During our simulations, the cylinder structure is directly followed by the optimized configuration. As illustration, we have shown in Fig. 7 some steps of

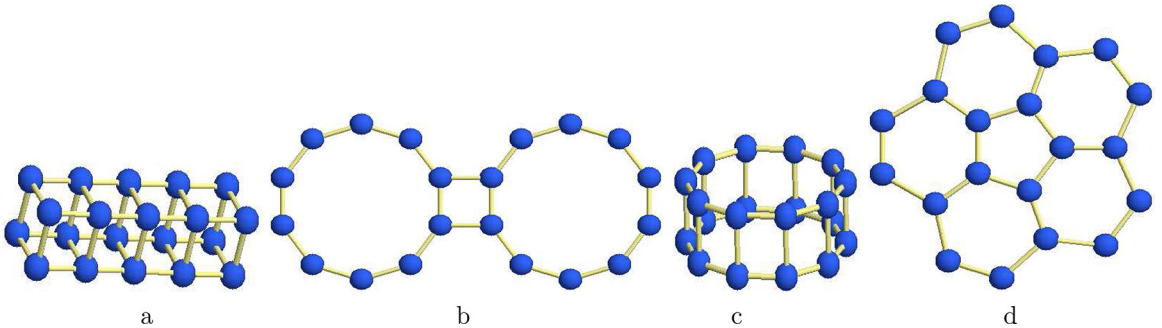

Fig. 5. Different initial configurations of Fe_{20}: (a) cage configuration, (b) butterfly configuration, (c) cylinder configuration, and (d) bowl configuration.

transformation of Fe_{20}, starting from a randomly initialized coordinates and velocities. The jumps observed here correspond to important modifications of structure.

4. Conclusion

The present work determines the optimized geometry as well as the ground state energy of iron clusters with up to 100 atoms. We have then determined the Gupta parameters for iron clusters. Comparison between our results with another published results has been carried out. We found that for $2 \leq N \leq 100$, the ground state energy of iron cluster obtained using Gupta potential decreases linearly with the number N of atoms. But the Fe–Fe bond fluctuates very slightly around $2.01256083r_0$ and the smallest value is $1.974096r_0$ for 65 atoms. Studying cluster interaction and cluster thermodynamic characteristics with the use of the technique developed are interesting themes which are left open for future considerations. It is also interesting to determine the magnetic moment of the optimized structures found in this paper.

References

[1] S. Goedecker, W. Hellmann, T. Lenosky, Phys. Rev. Lett. 95 (2005) 55501.
[2] P. Entel, M.E. Gruner, G. Rollmann, A. Hucht, S. Sahoo, A.T. Zayak, H.C. Herper, A. Dannenberg, Philos. Mag. 88 (2008) 2725.
[3] H. Dai, A. Rinzler, P. Nikolaev, A. Thess, D.T. Colbert, R.E. Smalley, Chem. Phys. Lett. 260 (1996) 471.
[4] J.A. Elliott, M. Hamm, Y. Shibuta, J. Chem. Phys. 130 (2009) 034704.
[5] R.S. Berry, D.J. Wales, Phys. Rev. Lett. 63 (1989) 1156.
[6] Y. Shibuta, T. Suzuki, Chem. Phys. Lett. 445 (2007) 265.
[7] I.M.L. Billas, A. Chatelain, W.A. deHeer, J. Magn. Magn. Mater. 168 (1997) 64.
[8] H.M. Cartwright, Applications of Evolutionary Computation Chemistry, Springer, 2004, and references therein.
[9] J. Holland, Adaptation in Natural and Artificial Systems, University of Michigan Press, Ann Arbor MI, USA, 1975.
[10] D.J. Wales, J.P.K. Doye, J. Phys. Chem. 101 (1997).
[11] H. Steven, S. Roger, Optimisation of carbon cluster geometry using a genetic algorithm, J. Chem. Soc. Faraday Trans. 93 (1997) 3919–3926.
[12] P.K.D. Jonathan, Lead clusters: different potentials, different structures, Comput. Mater. Sci. 35 (2006) 227–231.
[13] M.B.N. Jean, J.C. Charlier, Optimization of C20 isomers structure IC-85, 2001, 16 pp.
[14] P.K.D. Jonathan, C. Florent, Entropic effects on the size dependence of cluster structure, Phys. Rev. Lett. 86 (2001) 3570–3573.
[15] J.A. Elliott, Y. Shibuta, D.J. Wales, Global minima of transition metal clusters described by Finnis–Sinclair potentials: a comparison with semi-empirical molecular orbital theory, Philos. Mag. 89 (34–36) (2009) 3311–3332.
[16] I.L. Garzón, K. Michaelian, M.R. Beltrán, A. Posada-Amarillas, P. Ordejón, E. Artacho, D. Sánchez-Portal, J.M. Soler, Lowest energy structures of gold nanoclusters, Phys. Rev. Lett. 81 (1998) 1600–1603.
[17] K. Michaelian, N. Rendón, I.L. Garzón, Structure and energetics of Ni, Ag and Au nanoclusters, Phys. Rev. B 60 (1999) 2000–2010.
[18] J.A. Reyes-Nava, I.L. Garzón, M.R. Beltrán, K. Michaelian, Melting of sodium clusters, Rev. Mex. Fis. 48 (2002) 450–456.
[19] J.M. Soler, I.L. Garzón, J.D. Joannopoulos, Structural patterns of unsupported gold clusters, Solid State Commun. 117 (2001) 621–625.
[20] F. Cleri, V. Rosato, Phys. Rev. B 48 (1993) 22.
[21] V. Rosato, M. Guillope, B. Legrand, Thermodynamical and structural properties of f.c.c. transition metals using a simple tight-binding model, Philos. Mag. A 59 (1989) 321–336.
[22] R.P. Gupta, Lattice relaxation at a metal surface, Phys. Rev. B 23 (1981) 62–65.
[23] V. Loup, Computer "experiments" on classical fluids. I. Thermodynamical properties of Lennard–Jones molecules, Phys. Rev. 159 (1967) 98–103.
[24] J.L. Chen, C.S. Wang, K.A. Jackson, M.R. Pederson, Phys. Rev. B 44 (1991) 6558.
[25] P. Calaminici, Chem. Phys. Lett. 387 (2004) 253.
[26] M. Castro, D.R. Salahub, Phys. Rev. B 49 (1994) 11842.
[27] P. Ballone, R.O. Jones, Chem. Phys. Lett. 233 (1995) 632.
[28] O. Dieguez, M.M.G. Alemany, C. Rey, P. Ordejon, L.J. Gallego, Phys. Rev. B 63 (2001) 205407.
[29] C. Kohler, G. Seifert, T. Frauenheim, Chem. Phys. 309 (2005) 23.
[30] G.L. Gutsev, C.W. Bauschlicher Jr., J. Phys. Chem. A 107 (2003) 7013.
[31] Q.M. Ma, Z. Xie, J. Wang, Y. Liu, Y.-C. Li, Solid State Commun. 142 (2007) 114.
[32] S. Yuan, Y. Kong, F. Wen, F. Li, J. Phys.: Condens. Matter 19 (2007) 466203.
[33] Y.C. Bae, H. Osanai, V. Kumar, Y. Kawazoe, Phys. Rev. B 70 (2004) 195413.